Properties of Dielectric-Loaded T-Septum Waveguides

R. R. MANSOUR, MEMBER, IEEE, AND
R. H. MACPHIE, SENIOR MEMBER, IEEE

Abstract —**The conservation of complex power technique is employed to analyze T-septum waveguides. The effect of dielectric loading on the cutoff frequency and the bandwidth is investigated. Numerical results are presented which show that loading the gap with dielectric not only improves the power handling capability of the structure but also increases its bandwidth.**

I. Introduction

T-septum waveguides have been proposed by Mazumder and Saha [1], [2] as an alternative to conventional ridge waveguides due to their favorable cutoff and bandwidth characteristics. With the use of the Ritz–Galerkin method, numerical results have been reported in [1] and [2] which show that T-septum waveguides offer a lower cutoff frequency and a much higher bandwidth than can be achieved by ridge waveguides.

More recently, Zhang and Joines [3] have also applied the Ritz–Galerkin method to analyze T-septum waveguides and reported results which do not compare favorably with those published in [2]. Their results showed that T-septum waveguides can even offer a much greater bandwidth than that predicted by Mazumder and Saha [2].

T-septum waveguides are potentially attractive for use in the design of low-pass harmonic filters for many applications where a wide stopband rejection is required. In practice, however, the gap is usually filled with a dielectric material [4] in order to ensure performance to the required power-handling capability. The effect of dielectric loading in ridge waveguides has been studied in [5]; its effect, however, on the properties of T-septum waveguides remains to be determined.

The aim of this paper is threefold: 1) to investigate the properties of dielectric-loaded T-septum waveguides, 2) to explain the reason for the discrepancy between the results published by Zhang and Joines [3] and those reported by Mazumder and Saha [2], and 3) to present an analysis of T-septum waveguides which is different from the analyses reported in [2] and [3].

II. Formulation

Fig. 1(a) shows a single T-septum waveguide with dielectric loading. Due to the symmetry around the y axis, only half of the structure, as shown in Fig. 2, needs to be analyzed. At cutoff, the discontinuity seen at plane AA' of Fig. 2 is basically a junction between a parallel-plate waveguide and a bifurcated waveguide with a septum of thickness t. By regarding the bifurcated waveguide as a generalized port, the scattering parameters of this discontinuity are given by [6], [7]

$$\mathbf{S}_{22} = (\mathbf{P}_2^\dagger + \mathbf{H}^\dagger \mathbf{P}_1^\dagger \mathbf{H})^{-1}(\mathbf{P}_2^\dagger - \mathbf{H}^\dagger \mathbf{P}_1^\dagger \mathbf{H}) \tag{1a}$$

$$\mathbf{S}_{12} = \mathbf{H}(\mathbf{I} + \mathbf{S}_{22}) \tag{1b}$$

$$\mathbf{S}_{21} = 2(\mathbf{P}_2^\dagger + \mathbf{H}^\dagger \mathbf{P}_1^\dagger \mathbf{H})^{-1}\mathbf{H}^\dagger \mathbf{P}_1^\dagger \tag{1c}$$

$$\mathbf{S}_{11} = \mathbf{H}\mathbf{S}_{22} - \mathbf{I} \tag{1d}$$

Manuscript received September 20, 1988; revised May 3, 1989.
R. R Mansour is with COM DEV Ltd., Cambridge, Ont., Canada N1R 7H6.
R. H. MacPhie is with the Department of Electrical Engineering, University of Waterloo, Waterloo, Ont., Canada N2L 3G1.
IEEE Log Number 8929906.

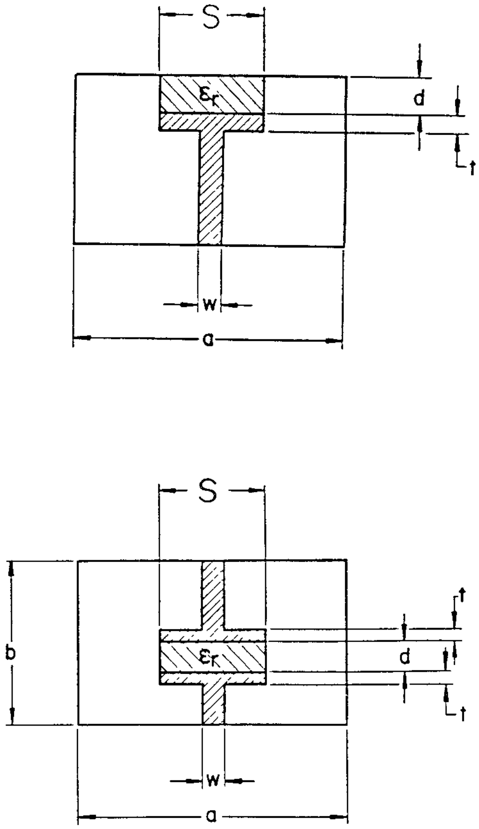

Fig. 1. Geometry of dielectric T-septum waveguide.

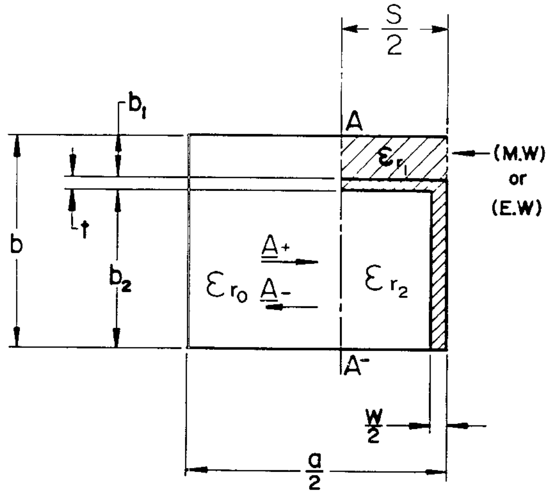

Fig. 2. Half of the cross section of a T-septum waveguide.

where $\mathbf{I}$ is the identity matrix, † denotes the Hermitian transpose, $\mathbf{H}$ is the E-field mode-matching matrix, and $\mathbf{P}_1$ and $\mathbf{P}_2$ are diagonal matrices whose diagonal elements are the power carried by unit-amplitude modes in the main guide and the bifurcated guide respectively. In view of [6], the elements of the matrices $\mathbf{H}$, $\mathbf{P}_1$, and $\mathbf{P}_2$ can be written as

$$\mathbf{H} = [\mathbf{H}_1 \quad \mathbf{H}_2] \qquad \mathbf{P}_2 = \begin{bmatrix} \mathbf{P}_{21} & \mathbf{0} \\ \mathbf{0} & \mathbf{P}_{22} \end{bmatrix}$$

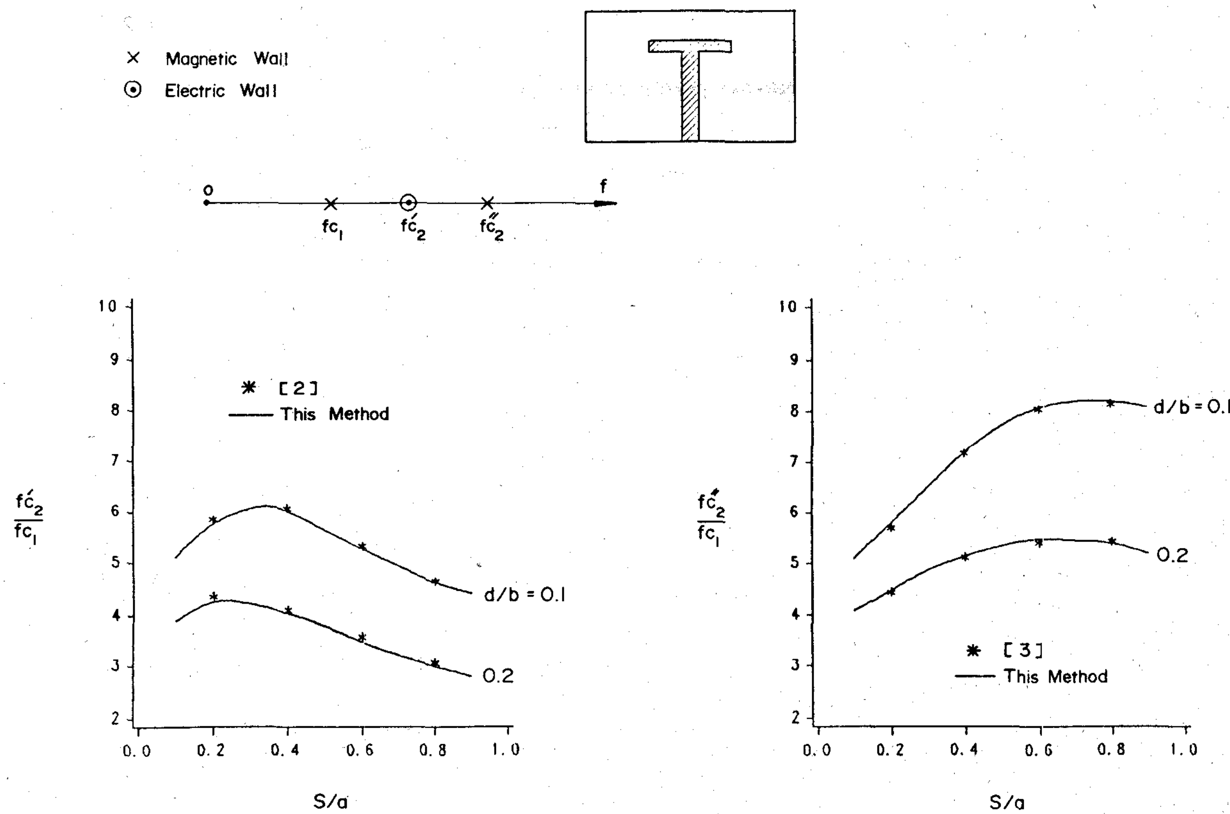

Fig. 3. Bandwidth characteristics: $b/a = 0.45$, $W/a = 0.1$, $t/b = 0.05$.

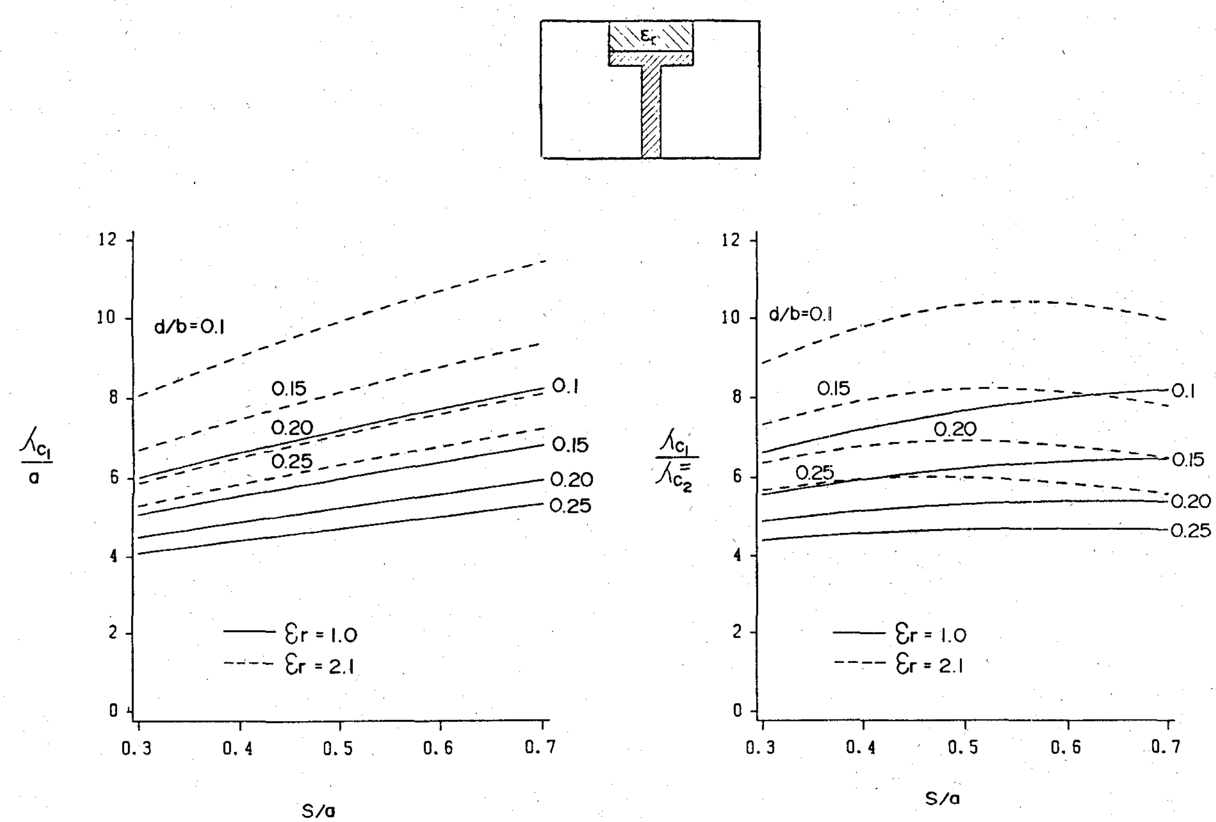

Fig. 4. Variation of bandwidth characteristics with S/a: $b/a = 0.45$, $W/a = 0.1$, $t/b = 0.05$.

where

$$H_{i,mn} = \begin{cases} \frac{m}{b} W_{i,mn}, & \frac{m}{b} \neq \frac{n}{b_i} \\ M_{i,m}, & \frac{m}{b} = \frac{n}{b_i} \\ & m,n = 0,1,2,\cdots \end{cases}$$

$$W_{i,mn} = \frac{\frac{2\pi}{b}}{\left(\frac{n\pi}{b_i}\right)^2 - \left(\frac{m\pi}{b}\right)^2} \left[(-1)^{n+1} \sin\left(\frac{m\pi}{b} h_i\right) + \sin\left(\frac{m\pi}{b} h_i'\right) \right]$$

$$M_{i,m} = \frac{b_i}{b} \cos\left(\frac{m\pi}{b} h_i'\right)$$

$$h_i = b \qquad h_i' = b - b_1 \qquad \text{for } i = 1$$

$$h_i = b_2 \qquad h_i' = 0 \qquad \text{for } i = 2$$

$$P_{1,nn} = \begin{cases} \frac{b}{2} \frac{\omega\epsilon_0}{\left[k_0^2 - \left(\frac{n\pi}{b}\right)^2\right]^{1/2}}, & n = 1,2,3,\cdots \\ b\left[\frac{\epsilon_0}{\mu_0}\right]^{1/2}, & n = 0 \end{cases}$$

and

$$P_{2i,nn} = \begin{cases} \frac{b_i}{2} \frac{\omega\epsilon_0\epsilon_{ri}}{\left[k_0^2\epsilon_{ri} - \left(\frac{n\pi}{b_i}\right)^2\right]^{1/2}}, & n = 1,2,3,\cdots \\ b_i\left[\frac{\epsilon_0\epsilon_{ri}}{\mu_0}\right]^{1/2}, & n = 0. \end{cases}$$

With the two waveguides of the bifurcated section terminated by electric and magnetic walls as illustrated in Fig. 2, it can be readily shown that the incident and reflected amplitude vectors $\boldsymbol{A}_+, \boldsymbol{A}_-$ defined at plane AA' are related by

$$\boldsymbol{A}_- = \mathbf{S}_r \boldsymbol{A}_+ \tag{2}$$

where

$$\mathbf{S}_r = \mathbf{S}_{11} + \mathbf{S}_{12}\mathbf{L}(\mathbf{I} - \mathbf{S}_{22}\mathbf{L})^{-1}\mathbf{S}_{21} \tag{3}$$

and

$$\mathbf{L} = \begin{bmatrix} \mathbf{L}_1 & \mathbf{0} \\ \mathbf{0} & \mathbf{L}_2 \end{bmatrix}. \tag{4}$$

$\mathbf{L}_1$ and $\mathbf{L}_2$ are diagonal matrices with diagonal elements given by

$$L_{1,nn} = \Gamma e^{-j\alpha_{1n}S} \tag{5a}$$

$$L_{2,nn} = -e^{-j\alpha_{2n}(S-W)} \tag{5b}$$

$$\alpha_{in} = \left(k_0^2\epsilon_{ri} - \left(\frac{n\pi}{b_i}\right)^2\right)^{1/2}, \qquad i = 0, 1, \text{ and } 2.$$

In (5a), $\Gamma = +1$ for magnetic wall symmetry and $\Gamma = -1$ for electric wall symmetry. Having determined $\mathbf{S}_r$, the eigenvalue equation for the cutoff frequency can then be written as

$$\det[\mathbf{I} + \mathbf{L}_0\mathbf{S}_r\mathbf{L}_0] = 0. \tag{6}$$

where $\mathbf{L}_0$ is a diagonal matrix with diagonal elements given by $L_{0,nn} = e^{-j\alpha_{0n}(a-S)/2}$. In addition to the simplicity of this analysis, it is numerically efficient: the pre and post multiplication of matrix $\mathbf{S}_r$ in (6) by the diagonal matrix $\mathbf{L}_0$, whose elements decay rapidly for large n, gives the eigenvalue equation a highly superior convergence property.

The solution for a symmetrical double T septum can be directly deduced from that of a single T septum by replacing b with $b/2$ and d with $d/2$. For an asymmetrical double T septum, the above analysis is still applicable; in this case, however, the discontinuity seen at plane AA' is a junction between a parallel-plate waveguide and a trifurcated waveguide. The scattering parameters for the trifurcated junction can be easily determined using [6]. It should be also mentioned that if we let $S = W$ in the above equations, the same formulation can be used to determine the characteristics of conventional single and double ridge waveguides.

III. Numerical Results and Discussion

The TE modes in T-septum waveguides can be classified into TE modes with magnetic wall symmetry (even modes) and TE modes with electric wall symmetry (odd modes). The dominant mode in these structures is a TE mode with magnetic wall symmetry. The typical spectrum of the first three TE modes in T-septum waveguides with $b/a = 0.45$ is illustrated in Fig. 3. In this figure, we also show the results calculated by the present analysis in comparison with those reported in [2] and [3]. It is clear that the discrepancy between the results reported in [2] and [3] lies basically in the definition used for the bandwidth: in [2] the bandwidth is defined as the ratio of the cutoff wavelength of the dominant mode to that of the first higher order mode, whereas it is defined in [3] as the ratio of the cutoff wavelength of the dominant mode to that of the first higher order even mode.

Although the definition used in [2] has been conventionally used for ridge waveguides [8], in many applications, such as filters and transformers, only modes with magnetic wall symmetry are excited and the guide exhibits a bandwidth according to [3]. It should, however, be noted that in comparing the achievable bandwidth of T-septum waveguides to that of ridge waveguides the same definition should be used. In the comparison given in [2, fig. 3] between the bandwidth of T-septum waveguides and that of ridge waveguides, the same definition is employed for both structures, whereas in [3, fig. 8] two different definitions are used.

In order to demonstrate the effect of dielectric loading, Fig. 4. shows the cutoff frequency and bandwidth of dielectric-loaded T-septum waveguides with different structure parameters. The results given in this figure for the bandwidth are based on the assumption that only modes with magnetic wall symmetry are excited. This figure also shows the calculated results for the same structure with $\epsilon_r = 1$. It is noted that with dielectric loading, the cutoff wavelength of the dominant mode increases with s/a and is always greater than the case with $\epsilon_r = 1$. It is also observed that while the cutoff wavelength of the dominant mode is considerably increased by dielectric loading, that of the higher order mode is slightly affected. This in turn leads to a considerable increase in the bandwidth, particularly for structures with small values of d/b. For example, the T-septum waveguide shown in Fig. 4 with $s/a = 0.5$, $d/b = 0.1$, and $\epsilon_r = 1$ exhibits a bandwidth of 7.66, whereas the same structure with $\epsilon_r = 2.1$ would exhibit a bandwidth of 10.35, about 35 percent higher than that obtained with $\epsilon_r = 1$.

In Table I we compare our results with the experimental results reported in [3]. It is observed that there is a good agreement. The effect of dielectric loading on the cutoff frequency and the bandwidth is also demonstrated in this table.

TABLE I
THE CUTOFF FREQUENCY AND BANDWIDTH OF A T-SEPTUM WAVEGUIDE

PARAMETERS	THIS METHOD $\varepsilon_r = 1.0$	MEASURED [3] $\varepsilon_r = 1.0$	CALCULATED [3] $\varepsilon_r = 1.0$	THIS METHOD $\varepsilon_r = 2.1$
Cutoff of dominant mode (MHz)	202	216	200	145
Cutoff of first higher order even mode (MHz)	1091	1092	1085	1087
Bandwidth	5.40	5.06	5.43	7 49

$a = 301.2$ mm, $b = 75.3$ mm, $S = 150.6$ mm, $t = 3.8$ mm, $d = 15.5$ mm, and $W = 30.1$ mm.

IV. CONCLUSIONS

A simple and numerically efficient analysis is presented for the characterization of dielectric-loaded T-septum waveguides. The validity of the analysis has been verified by comparing the calculated results with other available data for empty T-septum waveguides. It has been demonstrated that loading the gap with a dielectric material leads to a significant improvement in the bandwidth.

ACKNOWLEDGMENT

The authors express their thanks to the management of COM DEV Ltd. for permission to publish this work.

REFERENCES

[1] G. G Mazumder and P. K Saha, "A novel rectangular waveguide with double T-septums," *IEEE Trans. Microwave Theory Tech.*, vol. MTT-33, pp. 1235–1238, Nov 1985.
[2] G. G. Mazumder and P. K. Saha, "Rectangular waveguide with T-shaped septa," *IEEE Trans. Microwave Theory Tech.*, vol. MTT-35, pp. 201–204, Feb. 1987.
[3] Y. Zhang and W. T. Joines, "Some properties of T-septum waveguides," *IEEE Trans. Microwave Theory Tech.*, vol. MTT-35, pp. 769–775, Aug. 1987.
[4] P F. Clancy, "Multipactor control in microwave space systems," *Microwave J.*, pp 77–83, Mar. 1978.
[5] G. Magerl, "Ridged waveguides with inhomogeneous dielectric-slab loading," *IRE Trans. Microwave Theory Tech*, vol. MTT-26, pp. 413–416, June 1978.
[6] R. R. Mansour and R. H. MacPhie, "Scattering at an *N*-furcated parallel plate waveguide junction," *IEEE Trans. Microwave Theory Tech.*, vol. MTT-33, pp. 830–835, Sept 1985.
[7] R. R. Mansour and R. H. MacPhie, "An improved transmission matrix formulation of cascaded discontinuities and its application to *E*-plane circuits," *IEEE Trans Microwave Theory Tech.*, vol. MTT-34, pp. 1490–1498, Dec. 1986.
[8] T. S. Saad, Ed., *Microwave Engineers' Handbook*, vol. 1. Delham, MA: Artech House, 1971.